

Review on the inclusive rare decays $B \rightarrow X_s \gamma$ and $B \rightarrow X_d \gamma$ in the Standard Model

Kay Bieri and Christoph Greub

Institut für Theoretische Physik, Universität Bern, CH-3012 Bern, Switzerland

Received: 17 October 2003 / Accepted: 24 October 2003 /
Published Online: 30 October 2003 – © Springer-Verlag / Società Italiana di Fisica 2003

Abstract. We review the NLL QCD calculations for the branching ratio of $B \rightarrow X_s \gamma$ in the SM. In particular, we emphasize the problem related to the definition of the charm quark mass which leads to a rather large uncertainty of the NLL predictions. The various steps needed for a NNLL calculation, in which the m_c issue can be settled, is also sketched. We briefly summarize the results of a calculation of the $\mathcal{O}(\alpha_s^2 n_f)$ corrections to $\text{BR}(B \rightarrow X_s \gamma)$, which was recently performed as a first step in the NNLL program. We then also briefly review the status of the photon energy spectrum and show the comparison with experimental data. Finally, we review the status of the CKM suppressed decay mode $B \rightarrow X_d \gamma$.

1 Introduction

In the Standard model (SM), rare B decays like $B \rightarrow X_s \gamma$ or $B \rightarrow X_s \ell^+ \ell^-$ are induced by one-loop diagrams, where virtual W bosons and up-type quarks are exchanged. In many extensions of the SM, there are additional contributions, where the SM particles in the loop are replaced by nonstandard ones, like charged Higgs bosons, gluinos, charginos etc. If the masses of these new particles are not heavier by many orders of magnitude than the heaviest SM particles, the new physics contributions to rare B meson decays are expected to be generically large. The sensitivity for nonstandard effects implies the possibility for an indirect observation of new physics, or allows to put limits on the masses and coupling parameters of the new particles.

It is obvious that it is only possible to fully exploit the new physics potential of these decays when both, precise measurements and precise theoretical SM calculations exist.

In the following we mainly concentrate on the decays $B \rightarrow X_s \gamma$ and $B \rightarrow X_d \gamma$, while the rare semileptonic decay $B \rightarrow X_s \ell^+ \ell^-$ is reviewed at this conference by T. Hurth [1]. There are experimental analyses of the branching ratio $\text{BR}(B \rightarrow X_s \gamma)$ by CLEO [2,3,4], ALEPH [5], BELLE [6], and BABAR [7] as shown in Fig. 1, leading to the world average [8]

$$\text{BR}(B \rightarrow X_s \gamma)_{\text{exp}} = (3.34 \pm 0.38) \times 10^{-4}.$$

In contrast to the exclusive rare decay $B \rightarrow K^* \gamma$, the inclusive counterpart $B \rightarrow X_s \gamma$ is theoretically much cleaner as no specific model is needed to describe the hadronic final state. Indeed, nonperturbative effects in the inclusive decay mode are well under control due to the heavy

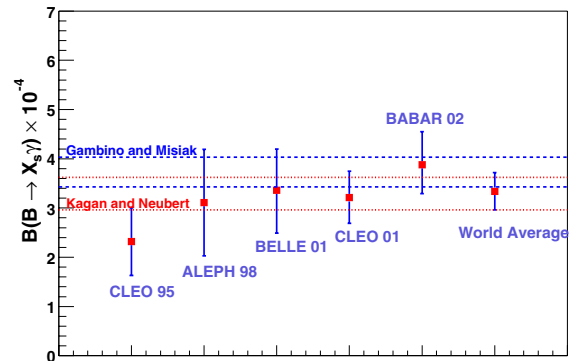


Fig. 1. Branching ratio $\text{BR}(B \rightarrow X_s \gamma)$: The numbers attached to the various experiments reflect the year of publication of the corresponding result. The dashed (dotted) band shows the theoretical results based on the $\overline{\text{MS}}$ (pole mass) interpretation of the charm quark mass; see (4) and (3). Figure taken from [7] and world average added from [8]

quark expansion technique (HQE), which implies that the decay width $\Gamma(B \rightarrow X_s \gamma)$ is well approximated by the partonic decay rate $\Gamma(b \rightarrow X_s \gamma)$ which can be analyzed in renormalization group improved perturbation theory. The (nonperturbative) power corrections which scale like $1/m_b^2$ [9] and $1/m_c^2$ [10] were estimated to be well below 10%.

2 Theoretical framework

Short distance QCD effects enhance the partonic decay rate $\Gamma(b \rightarrow s \gamma)$ by more than a factor of two. Analytically, these QCD corrections contain large logarithms of the

form $\alpha_s^n(m_b) \ln^m(m_b/M)$, where $M = m_t$ or $M = m_W$ and $m \leq n$ (with $n = 0, 1, 2, \dots$). In order to get a reasonable prediction for the decay rate, it turns out that one has to resum both, the leading-log (LL) terms ($m = n$) as well as the next-to-leading-log (NLL) terms ($m = n - 1$).

To achieve the necessary resummations, one usually constructs in a first step an effective low-energy theory and then resums the large logarithms by renormalization group techniques. The low energy theory is obtained by integrating out the heavy particles which in the SM are the top quark and the W -boson. The resulting effective Hamiltonian relevant for $b \rightarrow s \gamma$ in the SM and many of its extensions reads

$$H_{\text{eff}}(b \rightarrow s \gamma) = -\frac{4G_F}{\sqrt{2}} \lambda_t \sum_{i=1}^8 C_i(\mu) O_i(\mu) \quad , \quad (1)$$

where $O_i(\mu)$ are local operators consisting of light fields, $C_i(\mu)$ are the corresponding Wilson coefficients, which contain the complete top- and W - mass dependence, and $\lambda_t = V_{tb}V_{ts}^*$ with V_{ij} being the CKM matrix elements. The CKM dependence globally factorizes, because we work in the approximation $\lambda_u = 0$.

In the basis introduced by Misiak [11], the operators read

$$\begin{aligned} O_1 &= (\bar{s}_L \gamma^\mu T^a c_L) (\bar{c}_L \gamma_\mu T^a b_L) \quad , \\ O_2 &= (\bar{s}_L \gamma^\mu c_L) (\bar{c}_L \gamma_\mu b_L) \quad , \\ O_7 &= \frac{e}{16\pi^2} m_b(\mu) \bar{s} \sigma^{\mu\nu} R b F_{\mu\nu} \quad , \\ O_8 &= \frac{g_s}{16\pi^2} m_b(\mu) \bar{s} \sigma^{\mu\nu} R T^a b G_{\mu\nu}^a \quad . \end{aligned} \quad (2)$$

As the Wilson coefficients of the QCD penguin operators O_3, \dots, O_6 are small, we do not list them here.

A consistent calculation for $b \rightarrow s \gamma$ at NLL precision requires three steps:

- 1) a matching calculation of the full standard model theory with the effective theory at the scale $\mu = \mu_W$ to order α_s^1 for the Wilson coefficients, where μ_W denotes a scale of order M_W or m_t ;
- 2) a renormalization group evolution of the Wilson coefficients from the matching scale μ_W down to the low scale $\mu_b = \mathcal{O}(m_b)$, using the anomalous-dimension matrix to order α_s^2 ;
- 3) a calculation of the matrix elements of the operators at the scale $\mu = \mu_b$ to order α_s^1 .

As all three steps are rather involved, a common effort of several independent groups was needed in order to calculate the NLL prediction for $\text{BR}(B \rightarrow X_s \gamma)$ [12, 13, 14, 15, 11, 16, 17, 18]. For a detailed summary of the various steps and intermediate results, we refer to the recent review by T. Hurth [19]. However, we would like to point out that the most difficult part, viz. the calculation of three-loop anomalous dimensions performed by Chetyrkin, Misiak and Münz in 1996 [11], was only confirmed very recently by Gambino, Gorbahn and Haisch [20]. Their paper also contains the three-loop mixing of the four-Fermi operators into O_9 , which is important for the process $B \rightarrow X_s \ell^+ \ell^-$.

During the completion of the NLL QCD corrections, also calculations of electroweak corrections were started [21, 22, 23]. At present, the corrections of order $\alpha_{\text{em}} \ln(\mu_b/M) [\alpha_s \ln(\mu_b/M)]^n$, as well as the subleading terms of order $\alpha_{\text{em}} [\alpha_s \ln(\mu_b/M)]^n$ [24] are systematically available.

3 NLL (and partial NNLL) results for $\text{BR}(B \rightarrow X_s \gamma)$

Combining NLL QCD corrections with the electroweak corrections just mentioned and also including the $1/m_b^2$ [9] and $1/m_c^2$ [10] power corrections, the branching ratio reads

$$\text{BR}(B \rightarrow X_s \gamma) = (3.32 \pm 0.14 \pm 0.26) \times 10^{-4} \quad , \quad (3)$$

where the first error reflects the dependence on the renormalization scale μ_b varied in the interval $m_b/2 \leq \mu_b \leq 2m_b$, while the second error reflects the error due to the uncertainties in the input parameters.

Among the input parameters the charm quark mass m_c plays a crucial role. The charm quark mass dependence only enters the prediction for the decay width at the NLL level, more precisely through the $\mathcal{O}(\alpha_s)$ correction to the matrix elements $\langle s \gamma | O_{1,2} | b \rangle$. Until recently, all authors used the pole mass value m_c^{pole} for the charm quark mass in numerical evaluations, leading to a branching ratio as specified in (3).

In 2001, however, Gambino and Misiak [25] pointed out that the $\overline{\text{MS}}$ -bar mass \overline{m}_c , normalized at $\mu \approx m_b/2$, could be the better choice, because the charm quark appears as an off-shell particle in the loop involved in the above mentioned matrix element with a typical virtuality of $m_b/2$. Using this interpretation, $\overline{m}_c/m_b = 0.22 \pm 0.04$ is substantially smaller than the value $m_c^{\text{pole}}/m_b = 0.29 \pm 0.02$ used in (3), leading to a branching ratio of [25, 26]

$$\text{BR}(B \rightarrow X_s \gamma) = (3.70 \pm 0.30) \times 10^{-4} \quad . \quad (4)$$

We would like to stress here that the above argument in favour of \overline{m}_c is an intuitive one. Formally, the difference between using m_c^{pole} or \overline{m}_c amounts to a NNLL effect at the level of the branching ratio. This means that a NNLL becomes necessary in order to unambiguously fix this issue.

Before sketching the NNLL program, we would like to stress that settling the m_c issue is also important when extracting bounds on new physics, based on NLL calculations [27, 28]. For example, in the type-II two-Higgs-doublet model, one obtains a bound from $b \rightarrow s \gamma$ on the charged Higgs boson mass of $m_H > 350$ GeV (99% C.L.) when using \overline{m}_c . When using on the other hand m_c^{pole} , the bound is $m_H > 280$ GeV (99% C.L.) [25].

Concerning the NNLL program, it is clear that in order to get a full NNLL QCD result for $\text{BR}(B \rightarrow X_s \gamma)$, all the three steps listed above have to be improved by one order in α_s . This means that three-loop matching calculations are needed, up to four-loop anomalous dimensions have to

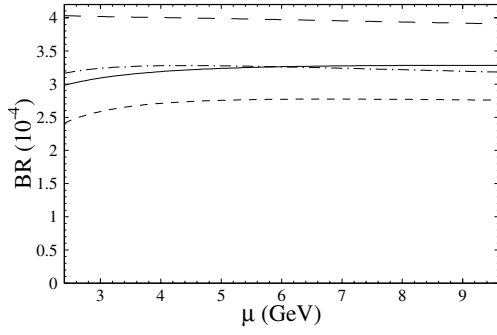


Fig. 2. $\text{BR}(B \rightarrow X_s \gamma)$ as a function of the renormalization scale μ . The dash-dotted curve shows the NLL prediction; the solid curve contains in addition the $\mathcal{O}(\alpha_s^2 n_f)$ terms. The long-dashed (short-dashed) curve is obtained by switching off the $\mathcal{O}(\alpha_s^2 n_f)$ corrections to O_7 (O_2). Figure taken from [29]

be worked out and up to three-loop calculations at the level of the matrix elements $\langle s\gamma | O_i(\mu_b) | b \rangle$ have to be performed. Several groups have been formed in order to attack this ambitious goal. Recently, a calculation of the $\mathcal{O}(\alpha_s^2 n_f)$ corrections to the matrix elements of the operators O_1 , O_2 , O_7 and O_8 was published [29]. Diagrammatically, these contributions are generated by inserting quark bubbles (n_f denotes the number of light quarks) into the gluon propagators in the diagrams which are involved in the calculations at NLL order. We note that these contributions are not related to the definition problem of m_c . However, in many other cases they are sources of large corrections. E.g., in the semileptonic decay width $\Gamma(B \rightarrow X_c \ell \nu_\ell)$ these $\mathcal{O}(\alpha_s^2 n_f)$ terms (after replacing $n_f \rightarrow -3\beta_0/2$, according to the procedure of naive non-abelianization) incorporate more than 80% of the complete $\mathcal{O}(\alpha_s^2)$ corrections [30]. The impact of the $\mathcal{O}(\alpha_s^2 n_f)$ corrections to $\text{BR}(B \rightarrow X_s \gamma)$ are shown in Fig. 2. The dash-dotted curve shows the NLL prediction, while the solid curve incorporates in addition the $\mathcal{O}(\alpha_s^2 n_f)$ terms (after the replacement $n_f \rightarrow -3\beta_0/2$, according to naive non-abelianization). As one sees from the figure, the $\mathcal{O}(\alpha_s^2 n_f)$ corrections seem to be small. Note, however, that this is a result of a relatively large accidental cancellation between corrections to O_2 and O_7 . This point is illustrated by the long-dashed and short-dashed curve, which are obtained by switching off the $\mathcal{O}(\alpha_s^2 n_f)$ corrections to O_7 and O_2 , respectively.

4 Partially integrated BR and photon energy spectrum

The photon energy spectrum of the partonic decay $b \rightarrow s\gamma$ is a delta function, concentrated at $\sim (m_b/2)$, when the b -quark decays at rest. This delta function gets smeared when considering the inclusive photon energy spectrum from a B meson decay. There is a perturbative contribution to this smearing, induced by the Bremsstrahlung process $b \rightarrow s\gamma g$ [16,17], as well as a nonperturbative one, which is due to the Fermi motion of the decaying b quark in the B meson.

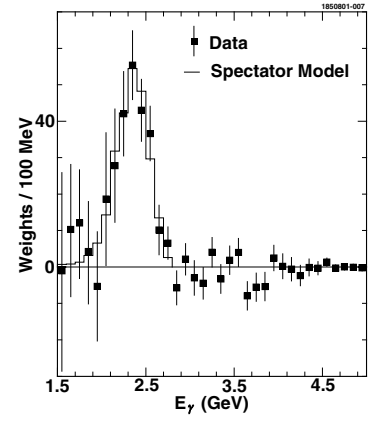


Fig. 3. Photon energy spectrum: The data points represent the CLEO measurement [4]. The histogram shows the theory result based on the spectator model using $p_F = 410$ MeV and $\langle m_b \rangle = 4.69$ GeV. Figure taken from [4]

For small photon energies, the γ -spectrum from $B \rightarrow X_s \gamma$ is completely overshadowed by background processes, like $b \rightarrow c\bar{u}d\gamma$ and $b \rightarrow u\bar{u}d\gamma$. This background falls off very rapidly with increasing photon energy, and becomes small for $E_\gamma > 2$ GeV [31]. This implies that only the partial branching ratio

$$\text{BR}(B \rightarrow X_s \gamma)(E_\gamma^{\min}) = \int_{E_\gamma^{\min}}^{E_\gamma^{\max}} \frac{d\text{BR}}{dE_\gamma} dE_\gamma \quad (5)$$

can be directly measured, with $E_\gamma^{\min} = \mathcal{O}(2)$ GeV.

Putting the energy cut at $E_\gamma^{\min} = 2.0$ GeV, CLEO used two methods to analyze their data on the photon energy spectrum in their most recent analysis: First, the Ali-Greub model [16,32], based on the spectator model formulated in [33] and second, methods based on HQET [22].

The spectator model contains two free parameters, viz. p_F , the average Fermi momentum of the b quark in the B meson and the mass of the spectator quark, m_{spec} . Equivalently $(p_F, \langle m_b \rangle)$ can be used as the free parameters, where $\langle m_b \rangle$ is the average b quark mass as defined in [16, 32]. In Fig. 3 a comparison between theory and experiment is shown. Using $p_F = 410$ MeV and $\langle m_b \rangle = 4.69$ GeV the best fit is obtained. We would like to stress that similar values for these parameters are also obtained when fitting the lepton spectra in $B \rightarrow X_c \ell \nu$ and $B \rightarrow X_u \ell \nu$.

A modern way - based on first principles - implements the Fermi motion in the framework of the heavy-quark expansion. When probing the spectrum closer to the endpoint, the OPE breaks down, and the leading twist non-perturbative corrections must be resummed into the B meson structure function $f(k_+)$ [34], where k_+ is the light-cone momentum of the b quark in the B meson. The physical spectrum is then obtained by the convolution

$$\frac{d\Gamma}{dE_\gamma} = \int_{2E_\gamma - m_b}^{\bar{\Lambda}} dk_+ f(k_+) \frac{d\Gamma_{\text{part}}}{dE_\gamma}(m_b^*) \quad , \quad (6)$$

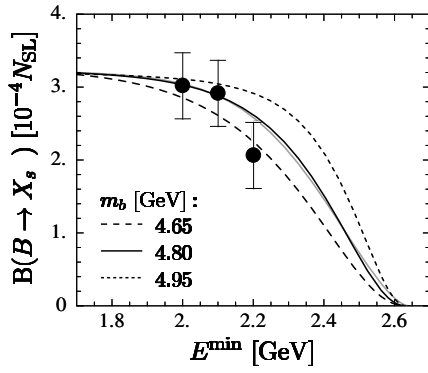


Fig. 4. Partially integrated branching ratio as a function of the energy cutoff E_γ^{\min} ; Curves taken from Kagan and Neubert [22]. Data point represent CLEO measurements [2,3,4]

where $(d\Gamma_{\text{part}}/dE_\gamma)(m_b^*)$ is the partonic differential rate, written as a function of the “effective mass” $m_b^* = m_b + k_+$. The function $f(k_+)$ has support in the range $-\infty < k_+ < \bar{\Lambda}$, where $\bar{\Lambda} = m_B - m_b$ in the infinite mass limit. This implies that the addition of the structure function moves the partonic endpoint of the spectrum from $m_b/2$ to the physical endpoint $m_B/2$. While the shape of the function $f(k_+)$ is unknown, the first few moments $A_n = \int dk_+ k_+^n f(k_+)$ are known: $A_0 = 1$, $A_1 = 0$ and $A_2 = -\lambda_1/3$. As A_n ($n > 2$) are poorly known, several Ansätze were used for $f(k_+)$; e.g. Neubert and Kagan [22] used $f(k_+) = N(1-x)^a e^{(1+a)x}$, with $x = k_+/\bar{\Lambda}$. Taking into account the constraints from A_0 , A_1 and A_2 , the independent parameters in this Ansatz can be chosen to be m_b and λ_1 . As shown in [22], the uncertainty of m_b dominates the error of the partial branching ratio. In Fig. 4 the partial branching ratio is shown for the relevant range of m_b as a function of E_γ^{\min} , keeping $\lambda_1/\bar{\Lambda}^2$ fixed. The data points show three CLEO measurements. In the oldest one the photon energy cut was put at $E_\gamma^{\min} = 2.2$ GeV, while in the most recent analysis this cut was lowered to 2.0 GeV, which is very important, because at 2.0 GeV the theoretical error on the partial branching ratio is considerably smaller, as seen from Fig. 4.

To determine from the measurement of the partial branching ratio the full BR, one needs from theory the fraction R of the $B \rightarrow X_s \gamma$ events with photon energies above E_γ^{\min} . Based on Kagan-Neubert [22], CLEO [4] obtained $R = (0.915_{-0.055}^{+0.027})$. A similar result is also obtained when using the spectator model.

It has been shown that up to corrections of $\mathcal{O}(\Lambda_{\text{QCD}}/m_b)$, the same shape function also describes $B \rightarrow X_u \ell \nu$ [35]. This implies that the photon energy spectrum can be used to predict the fraction of $B \rightarrow X_u \ell \nu$ events with $E_{\text{lept}} > 2.2$ GeV, where leptons coming from $B \rightarrow X_c \ell \nu$ are absent for kinematical reasons. Taking into account perturbative and Λ_{QCD}/m_b corrections [36,37,38], it is possible to extract V_{ub} from a measurement of the $B \rightarrow X_u \ell \nu$ decay rate in the region above 2.2 GeV. CLEO used this strategy in [39] to extract the CKM matrix element $|V_{ub}|$, obtaining $|V_{ub}| = (4.08 \pm 0.56_{\text{exp}} \pm 0.29_{\text{th}}) \times 10^{-3}$.

5 $B \rightarrow X_d \gamma$ in the SM

The decay $B \rightarrow X_d \gamma$ can be treated in a similar way as $B \rightarrow X_s \gamma$ [40]. The only difference is that λ_u for $b \rightarrow d \gamma$ is not small relative to λ_t and λ_c ; therefore, also the current-current operators O_1^u and O_2^u , weighted by λ_u , contribute.

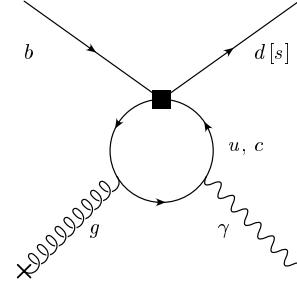


Fig. 5. Interaction of the c - and u -quark loop with soft gluons surrounding the b quark in the B meson

Unfortunately, these operators induce long-distance contributions to $B \rightarrow X_d \gamma$, which at present are not very well understood. To illustrate the problem, we first look at the corresponding charm quark loop, depicted in Fig. 5. In this case, one can expand the loop function

$$\sim \int_0^1 dx \int_0^{1-x} dy \frac{xy}{m_c^2 \left[1 - \frac{k_g^2}{m_c^2} x(1-x) - 2xy \frac{k_g k_\gamma}{m_c^2} \right]}$$

in powers of $t = k_g k_\gamma / m_c^2$, where k_g and k_γ denote the momentum of the gluon and the photon, respectively. This expansion generates the so-called Voloshin terms [10], which in $\text{BR}(B \rightarrow X_s \gamma)$ are a 3% effect. Obviously, there is no such OPE in the case of the u -quark loop. However, Buchalla, Isidori and Rey [41] argued that an expansion in $1/t$ can be done, leading to non-local operators. From naive dimensional counting, the leading contribution is expected to be of order Λ_{QCD}/m_b .

In reference [40], where NLL calculations for the process $B \rightarrow X_d \gamma$ were presented, the uncertainties due to the long-distance effects were absorbed into the theoretical error. Using $\mu_b = 2.5$ GeV and the central values of the input parameters, the analysis in reference [40] yields a difference between the LL and NLL predictions for $\text{BR}(B \rightarrow X_d \gamma)$ of $\sim 10\%$, increasing the branching ratio in the NLL case. For a fixed value of the CKM-Wolfenstein parameters ρ and η , the theoretical uncertainty of the average branching ratio $\langle \text{BR}(B \rightarrow X_d \gamma) \rangle$ of the decay $B \rightarrow X_d \gamma$ and its charge conjugate $\bar{B} \rightarrow \bar{X}_d \gamma$ is: $\Delta \langle \text{BR}(B \rightarrow X_d \gamma) \rangle / \langle \text{BR}(B \rightarrow X_d \gamma) \rangle = \pm(6-10)\%$. Of particular theoretical interest for constraining ρ and η is the ratio of the branching ratios, defined as

$$R(d\gamma/s\gamma) \equiv \frac{\langle \text{BR}(B \rightarrow X_d \gamma) \rangle}{\langle \text{BR}(B \rightarrow X_s \gamma) \rangle}, \quad (7)$$

in which a good part of the theoretical uncertainties cancels. Varying the CKM-Wolfenstein parameters ρ and η

in the range $-0.1 \leq \rho \leq 0.4$ and $0.2 \leq \eta \leq 0.46$ and taking into account other parametric dependences, the results (without electroweak corrections) are

$$6.0 \times 10^{-6} \leq \text{BR}(B \rightarrow X_d \gamma) \leq 2.6 \times 10^{-5}, \\ 0.017 \leq R(d\gamma/s\gamma) \leq 0.074.$$

Another observable, which is also sensitive to the CKM parameters ρ and η , is the CP rate asymmetry a_{CP} , defined as

$$a_{\text{CP}} = \frac{\Gamma(B \rightarrow X_d \gamma) - \Gamma(\bar{B} \rightarrow \bar{X}_d \gamma)}{\Gamma(B \rightarrow X_d \gamma) + \Gamma(\bar{B} \rightarrow \bar{X}_d \gamma)}. \quad (8)$$

Varying ρ and η in the range specified above, one gets $7\% \leq a_{\text{CP}} \leq 35\%$ [40]. We would like to point out that a_{CP} is at the moment only available to LL precision and therefore suffers from a relatively large renormalization scale dependence.

In summary, this decay mode is very challenging, both in theory and experiment: On the theory side more work is needed concerning the nonperturbative contributions associated with the u -quark loop, while on the experimental side the observation of this decay needs high statistics and a very good discrimination between pions and kaons.

Acknowledgements. This work is partially supported by the Swiss National Foundation and by RTN, BBW-Contract N0. 01.0357 and EC-Contract HPRN-CT-2002-00311 (EURIDICE).

References

1. T. Hurth, these proceedings
2. M.S. Alam et al. (CLEO Collab.), Phys. Rev. Lett. **74**, 2885 (1995)
3. S. Ahmed et al. (CLEO Collab.), CLEO CONF 99-10, hep-ex/9908022
4. S. Chen et al. (CLEO Collab.), Phys. Rev. Lett. **87**, 251807 (2001), hep-ex/0108032
5. R. Barate et al. (ALEPH Collab.), Phys. Lett. B **429**, 169 (1998)
6. K. Abe et al. (BELLE Collab.), Phys. Lett. B **511**, 151 (2001) hep-ex/0103042.
7. B. Aubert et al. (BABAR Collab.), hep-ex/0207074 and hep-ex/0207076
8. C. Jessop, SLAC-PUB-9610.
9. A. Falk, M. Luke, and M. Savage, Phys. Rev. D **49**, 3367(1994); I.I. Bigi, M. Shifman, N.G. Uraltsev, and A.I. Vainshtein, Phys. Rev. Lett. **71** (1993) 496; A.V. Manohar and M.B. Wise, Phys. Rev. D **49**, 1310(1994); A. Falk, M. Luke, and M. Savage, Phys. Rev. D **53**, 2491 (1996)
10. M.B. Voloshin, Phys. Lett. B **397**, 275 (1997); Z. Ligeti, L. Randall, and M.B. Wise, Phys. Lett. B **402**, 178 (1997); A.K. Grant, A.G. Morgan, S. Nussinov, and R.D. Peccei, Phys. Rev. **56**, 3151 (1997)
11. K. Chetyrkin, M. Misiak and M. Münz, Phys. Lett. B **400**, 206 (1997).
12. M. Ciuchini, E. Franco, G. Martinelli, L. Reina and L. Silvestrini, Phys. Lett. B **316**, 127 (1993); Nucl. Phys. B **415**, 403 (1994); G. Cella, G. Curci, G. Ricciardi and A. Vicere, Phys. Lett. B **325**, 227 (1994)
13. K. Adel and Y.-P. Yao, Phys. Rev. D **49**, 4945 (1994)
14. C. Greub and T. Hurth, Phys. Rev. D **56**, 2934 (1997)
15. A.J. Buras, A. Kwiatkowski and N. Pott, Nucl. Phys. B **517**, 353 (1998); Phys. Lett. B **414**, 157 (1997), E:ibid. **434**, 459 (1998)
16. A. Ali and C. Greub, Z. Phys. C **49**, 431 (1991); Phys. Lett. B **259**, 182 (1991)
17. N. Pott, Phys. Rev. D **54**, 938 (1996)
18. C. Greub, T. Hurth, and D. Wyler, Phys. Lett. B **380**, 385 (1996); Phys. Rev. D **54**, 3350 (1996)
19. T. Hurth, [arXiv:hep-ph/0212304]
20. P. Gambino, M. Gorbahn, and U. Haisch, [arXiv:hep-ph/0306079]
21. A. Czarnecki and W.J. Marciano, Phys. Rev. Lett. **81**, 277 (1998)
22. A.L. Kagan and M. Neubert, Eur. Phys. J. C **7**, 5 (1999)
23. K. Baranowski and M. Misiak, Phys. Lett. B **483**, 410 (2000) [arXiv:hep-ph/9907427].
24. P. Gambino and U. Haisch, JHEP **0009**, 001 (2000); P. Gambino and U. Haisch, JHEP **0110**, 020 (2001)
25. P. Gambino and M. Misiak, Nucl. Phys. B **611**, 338 (2001)
26. A.J. Buras, A. Czarnecki, M. Misiak, and J. Urban, Nucl. Phys. B **631**, 219 (2002)
27. M. Ciuchini, G. Degrassi, P. Gambino, and G.F. Giudice, Nucl. Phys. B **527**, 21 (1998)
28. F. M. Borzumati and C. Greub, Phys. Rev. D **58**, 074004 (1998); Phys. Rev. D **59**, 057501 (1998)
29. K. Bieri, C. Greub and M. Steinhauser, Phys. Rev. D **67**, 114019 (2003) [arXiv:hep-ph/0302051]
30. A. Czarnecki and K. Melnikov, Phys. Rev. D **59**, 014036 (1999)
31. A. Ali and C. Greub, Phys. Lett. B **293**, 226 (1992)
32. A. Ali and C. Greub, Z. Phys. C **49**, 431 (1991); Phys. Lett. B **259**, 182 (1991); Phys. Lett. B **361**, 146 (1995)
33. G. Altarelli et al., Nucl. Phys. B **208**, 365 (1982); A. Ali and E. Pietarinen, Nucl. Phys. B **154**, 519 (1979)
34. M. Neubert, Phys. Rev. D **49**, 3392 and 4623 (1994); I.I. Bigi, M.A. Shifman, N.G. Uraltsev and A.I. Vainshtein, Int. J. Mod. Phys. A **9**, 2467 (1994); R. D. Dikeman, M. Shifman and N.G. Uraltsev, Int. J. Mod. Phys. A **11**, 571 (1996); T. Mannel and M. Neubert, Phys. Rev. D **50**, 2037 (1994)
35. M. Neubert, Phys. Rev. D **49**, 4623 (1994) [arXiv:hep-ph/9312311]
36. A.K. Leibovich, I. Low, and I.Z. Rothstein, Phys. Rev. D **61**, 053006 (2000) [arXiv:hep-ph/9909404]
37. C.W. Bauer, M. Luke, and T. Mannel, Phys. Lett. B **543**, 261 (2002) [arXiv:hep-ph/0205150]
38. M. Neubert, Phys. Lett. B **543**, 269 (2002) [arXiv:hep-ph/0207002].
39. A. Bornheim et al. [CLEO Collaboration], Phys. Rev. Lett. **88**, 231803 (2002) [arXiv:hep-ex/0202019]
40. A. Ali, A. Asatrian and C. Greub, Phys. Lett. B **429**, 87 (1998)
41. G. Buchalla, G. Isidori and S.J. Rey, Nucl. Phys. B **511**, 594 (1998)